

Review

A Review of Molecular-Level Mechanism of Membrane Degradation in the Polymer Electrolyte Fuel Cell

Takayoshi Ishimoto¹ and Michihisa Koyama^{1,2,*}

¹ INAMORI Frontier Research Center, Kyushu University, 744 Motooka, Nishi-ku, Fukuoka 819-0395, Japan; E-Mail: ishimoto@ifrc.kyushu-u.ac.jp

² International Institute for Carbon-Neutral Energy Research, Kyushu University, 744 Motooka, Nishi-ku, Fukuoka 819-0395, Japan

* Author to whom correspondence should be addressed; E-Mail: koyama@ifrc.kyushu-u.ac.jp; Tel.: +81-92-802-6968; Fax: +81-92-802-6968.

Received: 30 April 2012; in revised form: 18 June 2012 / Accepted: 27 June 2012 /

Published: 10 July 2012

Abstract: Chemical degradation of perfluorosulfonic acid (PFSA) membrane is one of the most serious problems for stable and long-term operations of the polymer electrolyte fuel cell (PEFC). The chemical degradation is caused by the chemical reaction between the PFSA membrane and chemical species such as free radicals. Although chemical degradation of the PFSA membrane has been studied by various experimental techniques, the mechanism of chemical degradation relies much on speculations from *ex-situ* observations. Recent activities applying theoretical methods such as density functional theory, *in situ* experimental observation, and mechanistic study by using simplified model compound systems have led to gradual clarification of the atomistic details of the chemical degradation mechanism. In this review paper, we summarize recent reports on the chemical degradation mechanism of the PFSA membrane from an atomistic point of view.

Keywords: polymer electrolyte fuel cell; perfluorosulfonic acid membrane; chemical degradation; molecular level analysis

1. Introduction

The polymer electrolyte fuel cell (PEFC) has attracted much interest as a promising power source for automobiles and cogeneration systems because of its high energy conversion efficiency with

environmental benefits. The PEFC system has already been commercialized for residential use under the common name of “Ene-Farm” in Japan in 2009 [1,2]. For larger penetration of PEFC into society, practical long-term operation with a drastic cost reduction is necessary. One of the problems is the durability of the membrane electrode assemble (MEA) [3–9]. Degradations of the Pt electrocatalyst and the membrane are the central issues of MEA degradation. Concerning the loss of electrochemical surface area by Pt dissolution and reprecipitation phenomena of the Pt electrocatalyst during the operation, review papers are to be found based on many studies [10–20]. Additionally, there are some review papers of membrane degradation for practical applications [21–23]. In this paper, we focus on the chemical degradation of the membrane in MEA from an atomistic view to facilitate the understanding of the chemical reaction mechanisms of the membrane.

2. Membrane Degradation in PFSA

Most of the membranes used in PEFC have a perfluorinated backbone and are modified to include sulfonic groups that facilitate the transport of protons. The requirements for an excellent membrane are high proton conductivity, as well as thermal and chemical stability. The commonly used membranes for PEFC are perfluorosulfonic acid (PFSA) polymers such as Nafion[®] (Dupont), Gore-Select (Gore), Aciplex (Asahi Kasei), Flemion (AsahiGlass), and Celtec-P (BASF). The degradation of PFSA polymers accounts for a large part of the overall performance degradation of MEA. An understanding of the degradation mechanism of PFSA is thus important in the development of durable MEA. The degradation of PFSA can be classified into three categories, *i.e.*, mechanical, thermal, and chemical degradations.

2.1. Mechanical Degradation

The mechanical degradation is caused by repetition of expansion and contraction associated with changes in wet and dry conditions. Long-term durability studies under various conditions have been reported in order to understand the performance decrease mechanism of PFSA under critical operating conditions [24–34]. Pozio *et al.* reported that the long-term operation at low humidification led to a decrease of the three-dimensional reaction zone due to ionomer degradation by dehydration of the membranes. Schmittinger and Vahidi pointed out the importance of water management in membranes. To carefully analyze the water in the membrane, observation techniques of liquid water in the membrane were proposed by using time-resolved neutron radiography and high resolution dynamics in-plane neutron imaging [35–38]. In addition, the water distribution in the membrane was analyzed by computational fluid dynamics [39,40]. The mechanical degradation of the membrane becomes clear gradually on analysis of the distribution of liquid water and the performance of MEA.

2.2. Thermal Degradation

The thermal degradation is caused by operations at freezing and high temperatures [41–49]. The most favorable working temperature of the PFSA membrane is usually around 80 °C to maintain a highly efficient operation. However, wide temperature range operation is required to use PEFC in various environments. Membrane degradation at sub-freezing temperature is one of the critical

issues [41–43]. It has been observed that freezing water on the PFSA membrane leads to degradation due to different densities and conditions of water and ice. In addition, recently high temperature operation above 100 °C has been targeted for faster electrochemical kinetics, easier water management, and for the improvement of CO tolerance. The development of high durable and proton conductive membrane is one of the most important research fields. Recently, various kinds of membranes with blends, such as poly(arylene ether sulfonate ketone)s (SPESKs), sulfonated polyimide membrane containing triazole group (SPI-8), and sulfonated polyethersulfone (SPES), have been proposed for high durable membranes for thermal degradation [50–59].

2.3. Chemical Degradation

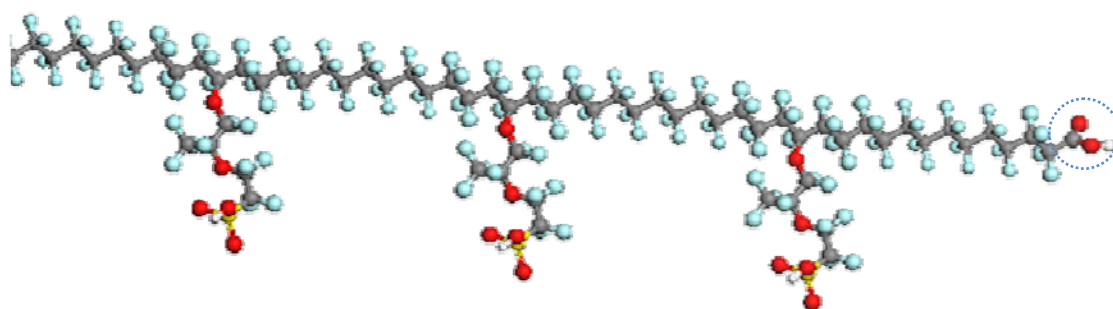
The chemical degradation is caused by the chemical reaction between membrane and chemical species. While mechanical and thermal degradation mechanisms can be understood macroscopically, atomistic understanding is essential for the chemical degradation mechanism. As a chemical species, it is generally believed that the degradation of PFSA membrane is caused by the attack of free radicals from hydrogen peroxide (H_2O_2) [60–78]. The H_2O_2 was confirmed in drain water, exhaust gas, and the membrane during operation of PEFCs. The H_2O_2 in PEFC is formed at the cathode from two-electron reduction of O_2 by cross-leakage of O_2 gas. The reactive hydroxyl ($\cdot OH$) and hydroperoxide ($\cdot OOH$) radicals are formed from H_2O_2 . Recently, the hydrogen radical ($\cdot H$) was also detected. Nosaka *et al.*, detected the OH radicals formed during the PEFC operation by a fluorescence probe method [62,63,65]. Although there are many experimental reports to analyze the OH formation mechanism [60,61,67,69–71,73], important knowledge is the chemical degradation of PFSA by radical species. This chemical degradation of PFSA is a microscopic phenomenon. It is necessary to analyze the chemical reaction between membrane and free radicals from an atomistic point of view. In the subsequent chapters, we summarize the recent studies clarifying the atomistic details of chemical degradation mechanisms of PFSA membrane using experimental and theoretical approaches.

3. Chemical Degradation Mechanism by Experiments

3.1. PFSA Main Chain

Figure 1 shows the structure of PFSA polymer, which consists of a perfluorinated main chain and a side chain including sulfonic groups as well as ether and C-S bonds.

Figure 1. Structure of Nafion[®] membrane.

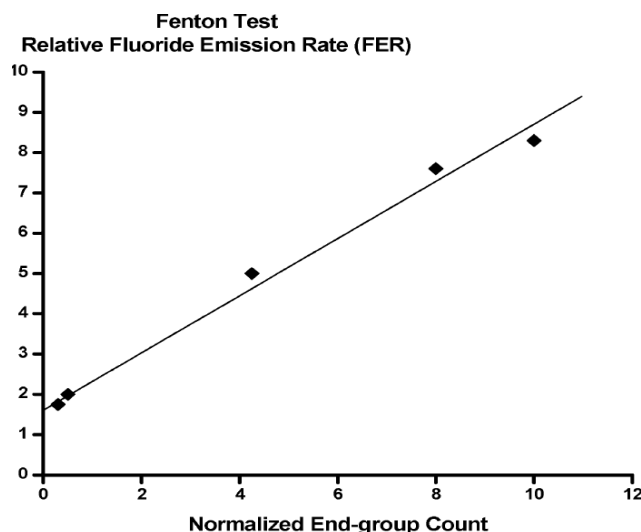


The degradation mechanism of free radical and carboxyl end groups has been examined by using Fenton's testing [79,80]. The chemical degradation of PFSA was explained by attack of the OH radical on the terminal $-\text{COOH}$ group in the perfluorinated main chain. This unzipping mechanism is shown below [81].



This mechanism indicates that the existence of the carboxylic (COOH) acid group in the perfluorinated main chain should be strongly related to the degradation of PFSA. This has been well-validated by plotting fluoride ion emission rate (FER) vs. carboxylic acid content in Nafion[®] (Figure 2), however, a decidedly non-zero intercept can be seen in Figure 2. At an extrapolated value of zero carboxylic acid groups in Nafion[®], over 10% of the total FER for untreated membrane remains [82,83]. This experimental result indicates the possibility of degradation by the attack of free radical except for the COOH group on the perfluorinated polymer main chain. Recently, the chemical degradation of the terminal carboxylic group in PFSA has not been the main issue of the chemical degradation, because several companies have addressed this problem by using original chemical stabilization procedures.

Figure 2. Plot showing relative fluoride emission rate (FER) from Fenton's test as a function of concentration of reactive end-groups (taken from in reference [82]).

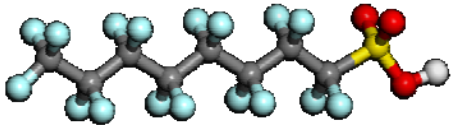
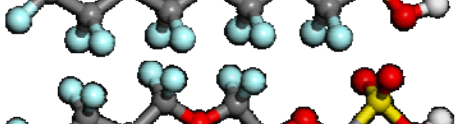
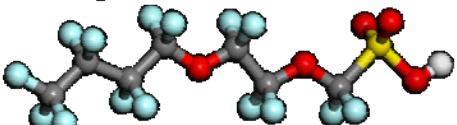
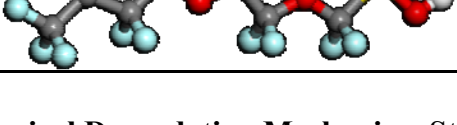


3.2. PFSA Side Chain

To explore the chemical degradation point in the PFSA membrane, Xie and Hayden analyzed the two possible PFSA chemical degradation mechanisms between the main chain end group and side chain [84]. From the IR spectra coupled with ionomer fluoride loss data, however, they found not only the carboxylic acid end group reaction of the main chain but also side chain cleavage reaction as PFSA chemical degradation pathways, whose contributions to overall degradation are difficult to quantitatively differentiate. To identify the degradation mechanism from the PFSA side chain, the

chemical degradation and stability of PFSA polymer against OH radical attack were investigated by solid-state NMR, solution NMR, and IR spectro-electrochemical methods [85–90]. Although some chemical species were detected by these analyses, the degradation mechanism was still unclear. Ishihara *et al.*, synthesized the model compounds of the PFSA main and side chains, $\text{CF}_3(\text{CF}_2)_8\text{SO}_3\text{H}$ and $\text{CF}_3(\text{CF}_2)_3\text{O}(\text{CF}_2)_2\text{OCF}_2\text{SO}_3\text{H}$, respectively, to explore the chemical degradation in the PFSA side chain [91]. They measured oxidative degradation of model compounds under the following Fenton test conditions: 100 °C, 15% H_2O_2 , catalyst $\text{FeSO}_4 \cdot 7\text{H}_2\text{O}$, and 6–24 h. The result of the degradation experiment in aqueous solution is shown in Table 1. The model compound representing the PFSA side chain was not fully recovered, although the one representing the main chain was completely recovered. This result clearly indicates that the PFSA side chain is vulnerable to OH radical attack. Recently, Dreilzer and Roduner also pointed out that the major point of OH radical attack is ether groups of the PFSA side chains, determined by using ESR measurement and reaction kinetics analysis [92].

Table 1. Experimental result of oxidative degradation reaction (taken from reference [91]).

Model compounds	Temperature (°C)	Time (h)	Recovery (%)
	100	6	100
	100	24	100
	100	6	84
	100	24	80

4. Chemical Degradation Mechanism Studied by Theoretical Methods

4.1. Theoretical Approaches for PFSA Membrane

Computational simulation is one of the most effective approaches for understanding chemical and physical phenomena. Computational fluid dynamics and multi scale modeling are often used for thermal and transportation analyses in MEA and optimization of PEFC performance [93–101]. Although these approaches have advantages for the analysis of macroscopic phenomena, the analysis of microscopic phenomena is necessary to utilize different types of computational simulations. First-principles calculations contribute to the analyses of detailed chemical reaction mechanisms from an atomistic point of view. There are many theoretical reports about hydration around the PFSA membrane and proton conductivity in PFSA membrane [102–109]. In addition, the proton conductivity due to proton transfer in the membrane was analyzed [110–118]. Physical properties, such as morphology, of membrane were also analyzed [119–125]. These theoretical results found that the proton dissociation from the membrane depends on the number of water molecules around the sulfonic acid, which is the end group of the PFSA side chain. Deprotonation from the sulfonic acid to the water solution becomes favorable as the number of water molecules around the sulfonic acid group increases. This trend led us to assume that the protonated and deprotonated sulfonic acid structures correspond to two extremes, *i.e.*, low and high humidity conditions. This is important information to understand on the structure of PFSA polymer. The analysis from an atomic point of view by first-principles calculation is effective to aid understanding of the chemical degradation mechanism of PFSA membrane.

4.2. Bond Dissociation Analysis

It is assumed that the degradation point of PFSA polymer by OH radical attack involves a relatively weak chemical bond in PFSA polymer. This information is useful in order to analyze the chemical degradation of PFSA polymer by OH radical attack based on the chemical reaction pathway analysis. One of the most useful applications is the analysis of bond dissociation energy. In fact, bond dissociation energy has been analyzed to understand the bond strength, bond character, and reactivity [126–135]. It was found that the C–F bond is relatively stronger than C–H. To identify the weak chemical bond in PFSA polymer, the estimation of bond dissociation energy in PFSA polymer is important. Coms carefully analyzed the C–F bond dissociation energies of various PFSA polymers containing C–O and C–S bonds [136]. He also analyzed the H and F abstraction energies by the OH radical. Based on these results of the thermochemical analysis, he confirmed the unzipping mechanism involving OH radical and pointed out the weak C–S bond including the PFSA side chain. Tokumasu *et al.*, analyzed the bond dissociation energy of the PFSA polymer side chain to provide some dissociation trends of the PFSA polymer [137]. The model structure they used is shown in Figure 3.

Figure 3. Molecular model of perfluorosulfonic acid (PFSA) polymer with atom labels (taken from reference [137]).

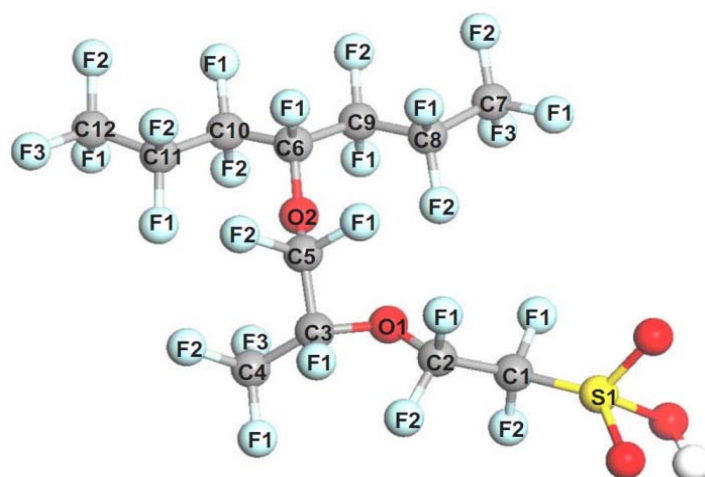


Table 2. Bond dissociation energy of the side chain backbone in the PFSA model (kJ/mol). Labels denote the bonds shown in Figure 3.

Bond	Neutral	Ionized
S1–C1	257.3	349.8
C1–C2	356.5	411.4
C2–O1	342.7	383.4
O1–C3	337.6	299.1
C3–C4	332.8	338.1
C3–C5	332.4	349.6
C5–O2	306.2	328.4
O2–C6	290.3	222.0

The C–F bonds in the side chain showed that the bond dissociation energy decreases in the order of primary, secondary, and tertiary bonds. The C–S bond was the weakest in the side chain backbone in the neutral molecule, which is a model for low humidity condition. When ionized PFSA polymer structure was used, a model for high humidity condition, the C–S bond became stronger. On the other hand, the C–O bond in the ionized structure became weaker than that in the neutral. These results indicate the different chemical degradation mechanisms of PFSA polymer under low and high humidity conditions. In addition, the C–O bond might be a degradation point with OH radical attack.

4.3. Degradation by Chemical Reaction of PFSA Polymer and OH Radical

Concerning the reactivity of the C–O bond by OH radical, there have been some studies with the first-principles calculation [138–143]. Based on these insights, we first theoretically analyzed the chemical degradation mechanism of the ether group in PFSA polymer model structures by the attack of OH radical [144]. We used the model structures $\text{CF}_3(\text{CF}_2)_3\text{O}(\text{CF}_2)_2\text{OCF}_2\text{SO}_3\text{H}$ representing the PFSA side chains because the experimental result by Ishihara *et al.*, suggested that the ether group in the PFSA side chain is vulnerable to OH radical attack. We performed a density functional theory (DFT) calculation to study the degradation reaction mechanism of the ether group in the model compound of the PFSA side chain with OH radical. The low and high humidity conditions of PFSA polymer side chain were represented by $\text{CF}_3(\text{CF}_2)_3\text{O}(\text{CF}_2)_2\text{OCF}_2\text{SO}_3\text{H}$ and $\text{CF}_3(\text{CF}_2)_3\text{O}(\text{CF}_2)_2\text{OCF}_2\text{SO}_3^-$, respectively. Figures 4 and 5 show the potential energy profile under high and low humidity conditions, respectively.

Figure 4. Potential energy profile under high humidity condition, $\text{CF}_3(\text{CF}_2)_3\text{O}(\text{CF}_2)_2\text{OCF}_2\text{SO}_3^- + \text{OH}$. The energy values (kJ/mol) are relative to reactants. Optimized structures of reactants, products, intermediate, and transition state are also shown in the potential energy profile. Important distances are shown in Å.

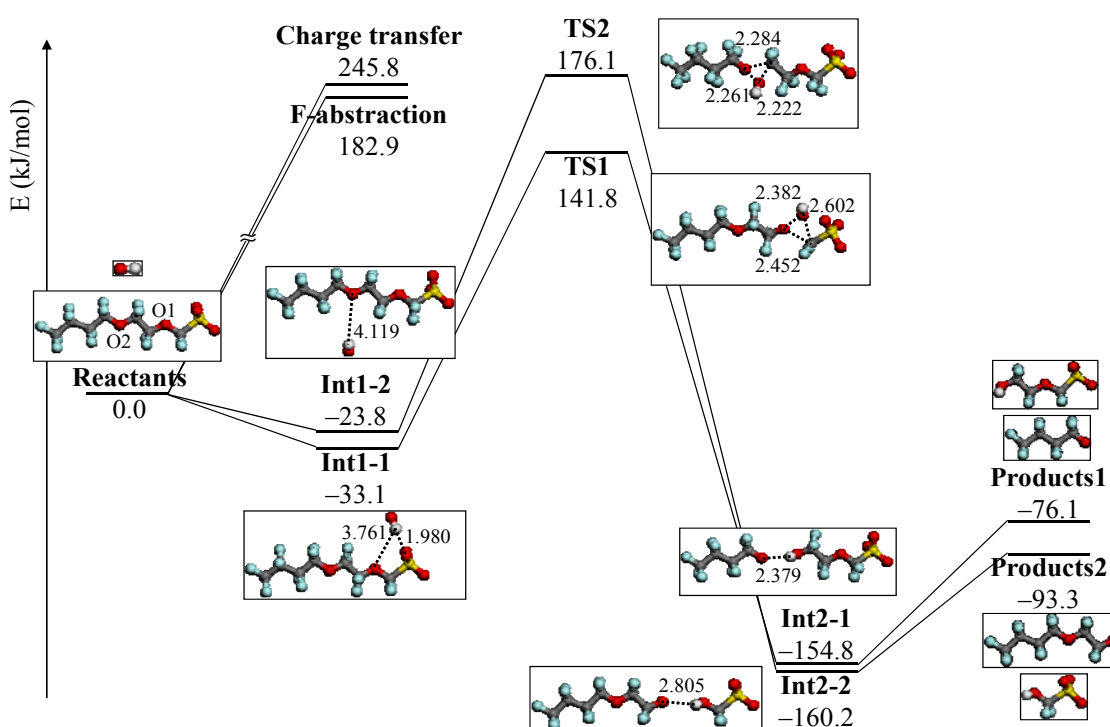
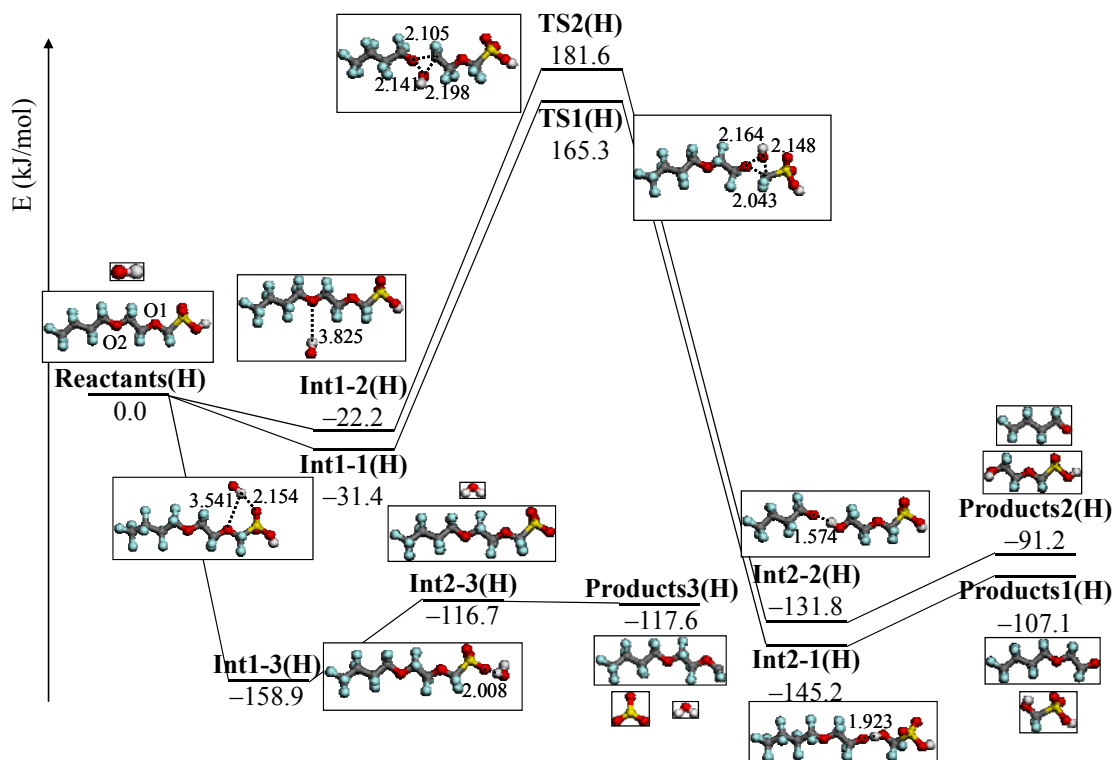


Figure 5. Potential energy profile under low humidity condition, $\text{CF}_3(\text{CF}_2)_3\text{O}(\text{CF}_2)_2\text{OCF}_2\text{SO}_3\text{H} + \cdot\text{OH}$. The energy values (kJ/mol) are relative to reactants. Optimized structures of reactants, products, intermediate, and transition state are also shown in the potential energy profile. Important distances are shown in Å.



Under high humidity condition, we clearly demonstrated the degradation mechanism and reactivity of C–O bond cleavage in the ether group by the OH radical. This result shows reasonable agreement with the experimental one. However, the OH radical prefers the reaction with the sulfonic acid group under the low humidity condition. We found a different reactivity of the OH radical under high and low humidity conditions.

Furthermore, we analyzed the chemical reaction pathways of PFSA side chain and OH radical by DFT calculations to study the degradation mechanism of the PFSA side chain [145]. The proton dissociated Nafion[®] was used as an example of PFSA polymer in the high humidity condition.

In this study, we calculated the reactivity between two ether groups in the Nafion[®] side chain and OH radical. The potential energy profile of the reaction is shown in Figure 6. The reactions of O1 and O2 in the Nafion[®] side chain attacked by the OH radical are denoted as reactions 1 and 2, respectively. Two reaction intermediate structures, Int1-1 and Int1-2, were obtained by weak attractive interaction between OH radical and O atoms in the ether groups. The stabilization energies of Int1-1 and Int1-2 were -34.6 and -14.1 kJ/mol, respectively. These intermediate compounds led to different products through the transition states. In the transition state, the C–O bond cleavage is induced by the OH radical in both cases. The energy of the C–O2 bond cleavage at TS2 was about 30 kJ/mol lower than that of C–O1 at TS1. We did not observe a difference in the chemical bond of the ether groups from the bond overlap population analyses. The atomic charges of O1 and O2 in the Nafion[®] side chain were -0.473 and -0.478 , respectively. Large stabilization was observed in Int1-1 because the O–H distance of Int1-1 is about 0.2 Å shorter than that of Int1-2. At the transition state, C–O1 and C–O2

bond distances in reactions 1 and 2 were 2.067 and 2.530 Å, respectively. This result indicates that the C–O2 bond cleavage at TS2 is favorable rather than C–O1 at TS1.

To discuss the difference of reactivity concerning the two ether groups with OH radical, we analyzed the ratio of the rate constants,

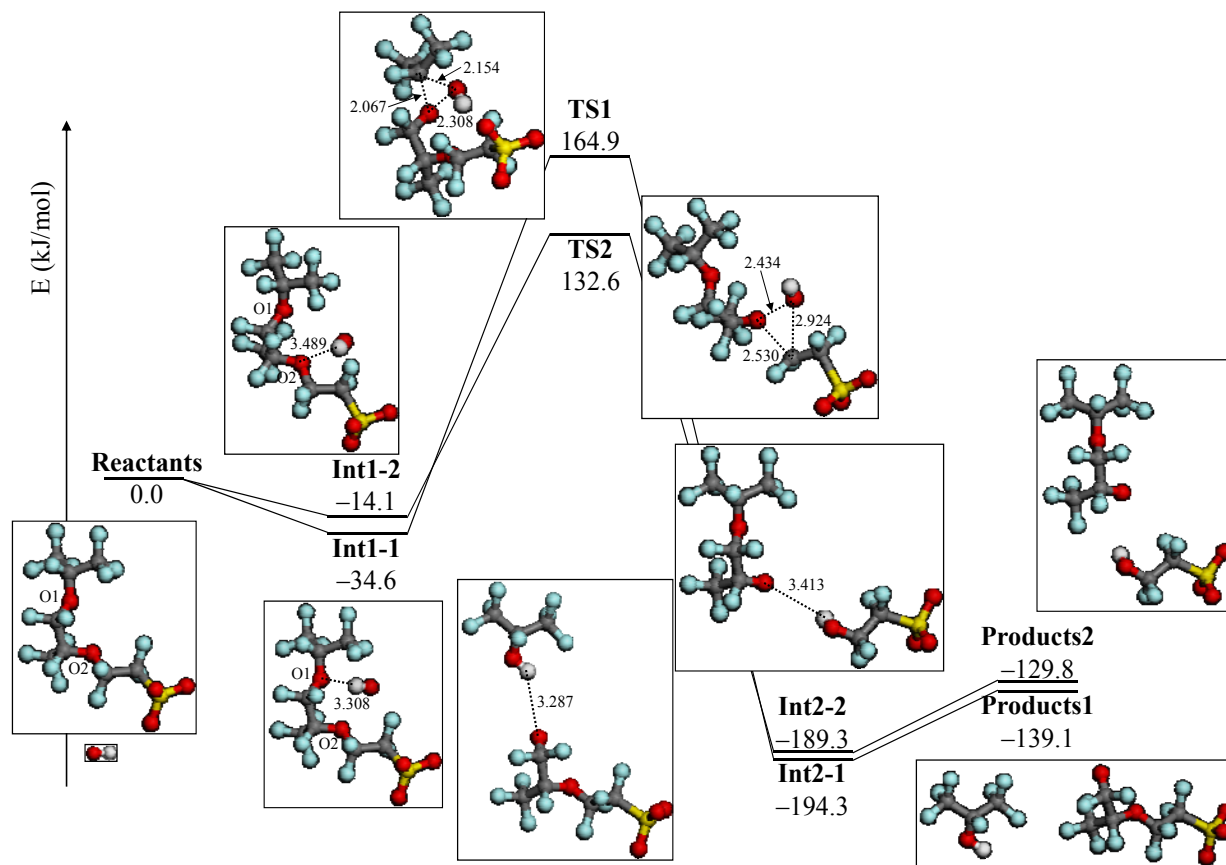


we evaluated the k_2/k_1 at 350 K using the following equation,

$$\frac{k_2}{k_1} = \exp\left(\frac{-(E_a^2 - E_a^1)}{RT}\right), \quad (6)$$

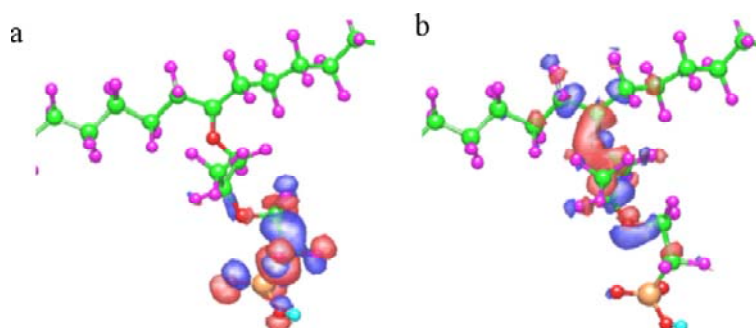
where the R and T are gas constant and temperature, respectively. The E_a^1 and E_a^2 are activation energies of reactions (4) and (5), respectively. Because k_2/k_1 is estimated as 4.0×10^3 , reaction (5) has a large advantage. We clearly demonstrated the degradation mechanism of the ether group in the Nafion[®] side chain by the OH radical from theoretical analysis as well as from the previous results for Nafion[®] model compounds.

Figure 6. Potential energy profile under high humidity condition, model structure of Nafion side chain +•OH. The energy values (kJ/mol) are relative to reactants. Optimized structures of reactants, products, intermediate, and transition state are also shown in the potential energy profile. Important distances are shown in Å.



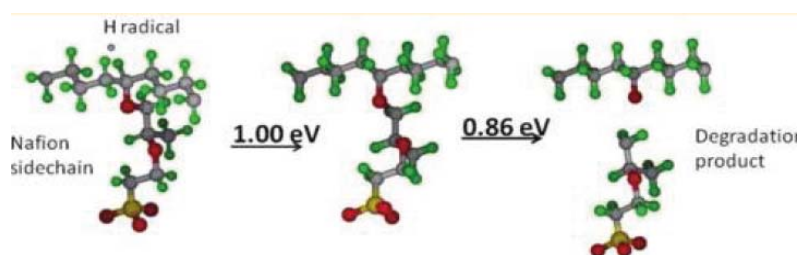
Uegaki *et al.*, analyzed the highest occupied molecular orbital (HOMO) and lowest unoccupied molecular orbital (LUMO) based on frontier orbital theory [146]. These orbitals play an important role to estimate electrophilic and nucleophilic reactions. The HOMO and LUMO in Nafion[®] are shown in Figure 7. The HOMO and LUMO are widely distributed around the terminal bond in the side chain and near main chain, respectively. They suggested that OH radical reacts around HOMO. Their expectation is similar to our analysis of the chemical degradation mechanism by C–O bond cleavage near the sulfonic acid group in the Nafion[®] side chain with OH radical. They also expected the reactivity around LUMO, which is near the main chain, by O₂^{•-} and H• species.

Figure 7. Optimized geometry of Nafion[®] and their molecular orbitals: (a) highest occupied molecular orbital (HOMO) and (b) lowest unoccupied molecular orbital (LUMO) (taken from reference [146]).



Furthermore, Yu *et al.*, showed another chemical degradation mechanism of the Nafion[®] side chain by OH radical [147]. They proposed two chemical mechanisms for OH radical attack on the Nafion[®] polymer: (1) OH radical attack on the S–C bond to form H₂SO₄ plus a carbon radical followed by decomposition of the carbon radical to form an epoxide; (2) OH radical attack on H₂ crossover gas to form a hydrogen radical, which subsequently attacks a C–F bond to form HF plus a carbon radical. This carbon radical can then decompose to form a ketone plus a carbon radical. The products (HF, OCF₂, SCF₂) from their proposed degradation mechanism have been observed by F NMR in the fuel cell [84].

Figure 8. Degradation mechanism of Nafion[®] proposed by Yu *et al.* (taken from reference [147]).



5. Summary

The degradation of PFSA can be classified into three categories, mechanical, thermal, and chemical. In this paper, we introduced recent studies on the chemical degradation of the PFSA membrane in

MEA from an atomistic view. The chemical degradation is caused by the chemical reaction between the PFSA membrane and chemical species. As regards the chemical species, it is generally believed that the degradation of PFSA membrane is caused by the attack of free radicals, such as OH radical from hydrogen peroxide. The OH radical was experimentally detected and the formation mechanism of OH radical investigated. The chemical degradation of PFSA membrane by the attack of OH radical can be classified into two degradation points. One is from the carboxylic group of the main chain, which is referred to as an unzipping mechanism, the other is from the side chain. Some experimental results suggested that one of the possible degradation points of the PFSA side chain is the ether group. However, detailed analysis of chemical degradation is not easy using only experimental techniques. Recently, computational analysis from an atomistic point of view has been gradually introduced. The chemical bond strengths of the Nafion[®] main and side chains were analyzed. The chemical degradation mechanism between the PFSA side chain and OH radical was rationalized by DFT calculations. The chemical degradation mechanism becomes clear from both molecular level experimental and theoretical analyses. After this breakthrough in the understanding of these chemical degradation mechanisms of the PFSA membrane, it is expected a durable membrane design of PEFC by combination of experimental and computational approaches will be achieved.

Acknowledgments

We are grateful for the financial support from KYOCERA corporation.

References

1. Fuel Cell Commercialization Conference of Japan Home Page. Available online: <http://www.fccj.jp> (accessed on 28 June 2012).
2. Staffell, I.; Green, R.J. Estimating future process for stationary fuel cells with empirically derived experience curves. *Int. J. Hydrog. Energy* **2009**, *34*, 5617–5628.
3. Vengatesan, S.; Fowler, M.W.; Yuan, X.Z.; Wang, H. Diagnosis of MEA degradation under accelerated relative humidity cycling. *J. Power Sources* **2011**, *196*, 5045–5052.
4. Lin, R.; Li, B.; Hou, Y.P.; Ma, J.M. Investigation of dynamic driving cycle effect on performance degradation and microstructure change of PEM fuel cell. *Int. J. Hydrog. Energy* **2009**, *34*, 2369–2376.
5. Shah, A.A.; Ralph, T.R.; Walsh, F.C. Modeling and simulation of the degradation of perfluorinated ion-exchange membranes in PEM fuel cells. *J. Electrochem. Soc.* **2009**, *156*, B465–B484.
6. Chen, C.; Fuller, T.F. XPS analysis of polymer membrane degradation in PEMFCs. *J. Electrochem. Soc.* **2009**, *156*, B1218–B1224.
7. Chen, C.; Fuller, T.F. The effect of humidity on the degradation of Nafion membrane. *Polym. Degrad. Stab.* **2009**, *94*, 1436–1447.
8. Ghassemzadeh, L.; Marrony, M.; Barrera, R.; Kreuer, K.D.; Maier, J.; Müller, K. Chemical degradation of proton conducting perfluorosulfonic acid ionomer membranes studied by solid-state nuclear magnetic resonance spectroscopy. *J. Power Sources* **2009**, *186*, 334–338.

9. Zhang, S.; Yuan, X.; Wang, H.; Mérida, W.; Zhu, H.; Shen, J.; Wu, S.; Zhang, J. A review of accelerated stress tests of MEA durability in PEM fuel cells. *Int. J. Hydrog. Energy* **2009**, *34*, 388–404.
10. Takizawa, S.; Nakazawa, A.; Inoue, M.; Umeda, M. Anodic Pt dissolution in concentrated trifluoromethanesulfonic acid. *J. Power Sources* **2010**, *195*, 5966–5970.
11. Yousfi-Steiner, N.; Moçotéguy, Ph.; Candusso, D.; Hissel, D. A review on polymer electrolyte membrane fuel cell catalyst degradation and starvation issues: Causes, consequences, and diagnostic for mitigation. *J. Power Sources* **2009**, *194*, 130–145.
12. Chung, C.G.; Kim, L.; Sung, Y.W.; Lee, J.; Chung, J.S. Degradation mechanism of electrocatalyst during long-term operation of PEMFC. *Int. J. Hydrog. Energy* **2009**, *34*, 8974–8981.
13. Kim, L.; Chung, C.G.; Sung, Y.W.; Chung, J.S. Dissolution and migration of platinum after long-term operation of a polymer electrolyte fuel cell under various conditions. *J. Power Sources* **2008**, *183*, 524–532.
14. Mitsushima, S.; Koizumi, Y.; Uzuka, S.; Ota, K. Dissolution of platinum in acidic media. *Electrochim. Acta* **2008**, *54*, 455–460.
15. Borup, R.M.; Meyers, J.; Pivovar, B.; Kim, Y.S.; Mukundan, R.; Garland, N.; Myers, D.; Wilson, M.; Garzon, F.; Wood, D.; Zelenay, P.; More, K.; Stroh, K.; Zawodzinski, T.; Boncella, J.; McGrath, J.E.; Inaba, M.; Miyatake, K.; Hori, M.; Ota, K.; Ogumi, Z.; Miyata, S.; Mishikata, A.; Siroma, Z.; Uchimoto, Y.; Yasuda, K.; Kimijima, K.; Iwashita, N. Scientific aspects of polymer electrolyte fuel cell durability and degradation. *Chem. Rev.* **2007**, *107*, 3904–3951.
16. Shao-Horn, Y.; Sheng, W.C.; Chen, S.; Ferreira, P.J.; Holby, E.F.; Morgan, D. Instability of supported platinum nanoparticles in low-temperature fuel cells. *Top. Catal.* **2007**, *46*, 285–305.
17. Yasuda, K.; Taniguchi, A.; Akita, T.; Ioroi, T.; Siroma, Z. Characteristics of a platinum black catalyst layer with regard to platinum dissolution phenomena in a membrane electrode assembly. *J. Electrochem. Soc.* **2006**, *153*, A1599–A1603.
18. Wang, X.; Kumar, R.; Myers, D.J. Effect of voltage on platinum dissolution. *Electrochem. Solid-State Lett.* **2006**, *9*, A225–A227.
19. Xie, J.; Wood, D.L., III; Wayne, D.M.; Zawodzinski, T.A.; Atanassov, P.; Borup, R.L. Durability of PEFCs at high humidity conditions. *J. Electrochem. Soc.* **2005**, *152*, A104–A113.
20. Antolini, E. Formation, microstructural characteristics and stability of carbon supported platinum catalysts for low temperature fuel cells. *J. Mater. Sci.* **2003**, *38*, 2995–3005.
21. Wu, J.; Yuan, X.Z.; Martin, J.J.; Wang, H.; Zhang, J.; Shen, J.; Wu, S.; Merida, W. A review of PEM fuel cell durability: Degradation mechanisms and mitigation strategies. *J. Power Sources* **2008**, *184*, 104–119.
22. Schmittinger, W.; Vahidi, A. A review of the main parameters influencing long-term performance and durability of PEM fuel cells. *J. Power Sources* **2008**, *180*, 1–14.
23. De Bruijn, F.A.; Dam, V.A.; Janssen, J.M. Review: Durability and degradation issues of PEM fuel cell components. *Fuel Cell* **2008**, *1*, 3–22.
24. Hartnig, C.; Schmidt, T.J. Simulated start-stop as a rapid aging tool for polymer electrolyte fuel cell electrodes. *J. Power Sources* **2011**, *196*, 5564–5572.

25. Scholta, J.; Pawlik, J.; Chmielewski, N.; Jörissen, L. Longevity test results for reformat polymer electrolyte membrane fuel cell stacks. *J. Power Sources* **2011**, *196*, 5264–5271.
26. Ishigami, Y.; Takada, K.; Yano, H.; Inukai, J.; Uchida, M.; Nagumo, Y.; Hyakutake, T.; Nishide, H.; Watanabe, M. Corrosion of carbon supports at cathode during hydrogen/air replacement at anode studied by visualization of oxygen partial pressures in a PEFC—Start-up/shut-down simulation. *J. Power Sources* **2011**, *196*, 3003–3008.
27. Pozio, A.; Cemmi, A.; Mura, F.; Masci, A.; Serra, E.; Silva, R.F. Long-term durability study of perfluoropolymer membranes in low humidification conditions. *J. Solid State Electrochem.* **2011**, *15*, 1209–1216.
28. Nakamura, S.; Kashiwa, E.; Sasou, H.; Hariyama, S.; Aoki, T.; Ogami, Y.; Nishikawa, H. Measurement of leak current generation distribution in PEFC and its application to load fluctuation testing under low humidification. *Elec. Eng. Jpn.* **2011**, *174*, 1–9.
29. Zhang, J.; Song, C.; Zhang, J. Accelerated lifetime testing for proton exchange membrane fuel cells using extremely high temperature and unusually high load. *J. Fuel Cell Sci. Technol.* **2011**, *8*, 051006:1–051006:5.
30. Bajpai, H.; Khandelwal, M.; Kumbur, E.C.; Mench, M.M. A computational model for assessing impact of interfacial morphology on polymer electrolyte fuel cell performance. *J. Power Sources* **2010**, *195*, 4196–4205.
31. Kim, J.H.; Jo, Y.Y.; Cho, E.A.; Jang, J.H.; Kim, H.J.; Lim, T.H.; Oh, I.H.; Ko, J.J.; Son, I.J. Effects of cathode inlet relative humidity on PEMFC durability during startup-shutdown cycling. *J. Electrochem. Soc.* **2010**, *157*, B633–B642.
32. Pinton, E.; Fourneron, Y.; Rosini, S.; Antoni, L. Experimental and theoretical investigations on a proton exchange membrane fuel cell starting up at subzero temperatures. *J. Power Sources* **2009**, *186*, 80–88.
33. Chen, J.; Zhai, M.; Asano, M.; Huang, L.; Maekawa, Y. Long-term performance of polyetheretherketone-based polymer electrolyte membrane in fuel cells at 95 °C. *J. Mater. Sci.* **2009**, *44*, 3674–3681.
34. Marrony, M.; Barrera, R.; Quenet, S.; Ginocchio, S.; Montelatici, L.; Aslanides, A. Durability study and lifetime prediction of baseline proton exchange membrane fuel cell under severe operating conditions. *J. Power Sources* **2008**, *182*, 469–475.
35. Oberholzer, P.; Boillat, P.; Siegrist, R.; Perego, R.; Kästner, A.; Lehmann, E.; Scherer, G.G.; Wokaun, A. Cold-start of a PEFC visualized with high resolution dynamics in-plane neutron imaging. *J. Electrochem. Soc.* **2012**, *159*, B235–B245.
36. Hickner, M.A.; Siegel, N.P.; Chen, K.S.; Hussey, D.S.; Jacobson, D.L. Observations of transient flooding in a proton exchange membrane fuel cell using time-resolved neutron radiography. *J. Electrochem. Soc.* **2010**, *157*, B32–B38.
37. Turhan, A.; Heller, K.; Brenizer, J.S.; Mench, M.M. Passive control of liquid water storage and distribution in a PEFC through flow-field design. *J. Power Sources* **2008**, *180*, 773–783.
38. Yu, J.; Matsuura, T.; Yoshikawa, Y.; Islam, M.N.; Hori, M. *In situ* analysis of performance degradation of a PEMFC under nonsaturated humidification. *Electrochem. Solid-State Lett.* **2005**, *8*, A156–A158.

39. Serincan, M.F.; Pasaogullari, U. Mechanical behavior of the membrane during the polymer electrolyte fuel cell operation. *J. Power Sources* **2011**, *196*, 1303–1313.
40. He, S.; Mench, M.M. One-dimensional transient model for frost heave in polymer electrolyte fuel cells. *J. Electrochem. Soc.* **2006**, *153*, A1724–A1731.
41. Park, G.G.; Lim, S.J.; Park, J.S.; Yim, S.D.; Park, S.H.; Yang, T.H.; Yoon, Y.G.; Kim, C.S. Analysis on the freeze/thaw cycled polymer electrolyte fuel cell. *Curr. Appl. Phys.* **2010**, *10*, 562–565.
42. Yang, X.G.; Tabuchi, Y.; Kagami, F.; Wang, C.Y. Durability of membrane electrode assemblies under polymer electrolyte fuel cell cold-start cycling. *J. Electrochem. Soc.* **2008**, *155*, B752–B761.
43. Kim, S.; Mench, M.M. Physical degradation of membrane electrode assemblies undergoing freeze/thaw cycling: Micro-structure effects. *J. Power Sources* **2007**, *174*, 206–220.
44. Carbone, A.; Saccá, A.; Busacca, C.; Frontera, P.; Antonucci, P.L.; Passalacqua, E. Nafion electro-spun reinforced membranes for polymer electrolyte fuel cell. *J. Nanosci. NanoTechnol.* **2011**, *11*, 8768–8774.
45. Zhang, Z.; Xie, Z.; Zhang, J.; Tang, Y.; Song, C.; Navessin, T.; Shi, Z.; Song, D.; Wang, H.; Wilkinson, D.P.; Liu, Z.S.; Holdcroft, S. High temperature PEM fuel cells. *J. Power Sources* **2006**, *160*, 872–891.
46. Collier, A.; Wang, H.; Yuan, X.Z.; Zhang, J.; Wilkinson, D.P. Degradation of polymer electrolyte membranes. *Int. J. Hydrog. Energy* **2006**, *31*, 1838–1854.
47. Savadogo, O. Emerging membranes for electrochemical systems: Part II. High temperature composite membranes for polymer electrolyte fuel cell (PEFC) applications. *J. Power Sources* **2004**, *127*, 135–161.
48. Yang, C.; Srinivasan, S.; Bocarsly, A.B.; Tulyani, S.; Benziger, J.B. A comparison of physical properties and fuel cell performance of Nafion and zirconium phosphate/Nafion composite membranes. *J. Membr. Sci.* **2004**, *237*, 145–161.
49. Ma, C.; Zhang, L.; Mukerjee, S.; Ofer, D.; Nair, B. An investigation of proton conduction in select PEM's and reaction layer interfaces-designed for elevated temperature operation. *J. Membr. Sci.* **2003**, *219*, 123–136.
50. Okanishi, T.; Tsuji, Y.; Sakiyama, Y.; Matsuno, S.; Bae, B.; Miyatake, K.; Uchida, M.; Watanabe, M. Effect of PEFC operating conditions on the durability of sulfonated poly(arylene ether sulfone ketone) multiblock membranes. *Electrochim. Acta* **2011**, *56*, 8989–8996.
51. Okanishi, T.; Tsuji, Y.; Sakiyama, Y.; Matsuno, S.; Bae, B.; Miyatake, K.; Uchida, M.; Watanabe, M. Effect of PEFC operating conditions on the durability of sulfonated polyimide membranes. *Electrochim. Acta* **2011**, *58*, 589–598.
52. Kabasawa, A.; Saito, J.; Miyatake, K.; Uchida, H.; Watanabe, M. Effects of the decomposition products of sulfonated polyimide and Nafion membranes on the degradation and recovery of electrode performance in PEFCs. *Electrochim. Acta* **2009**, *54*, 2754–2760.
53. Kabasawa, A.; Saito, J.; Yano, H.; Miyatake, K.; Uchida, H.; Watanabe, M. Durability of a novel sulfonated polyimide membrane in polymer electrolyte fuel cell operation. *Electrochim. Acta* **2009**, *54*, 1076–1082.
54. Kerres, J. Blend concepts for fuel cell membranes. *Polym. Membr. Fuel Cells* **2009**, *10*, 185–210.

55. Kang, M.S.; Lee, M.J. Anhydrous solid proton conductors based on perfluorosulfonic ionomer with polymeric solvent for polymer electrolyte fuel cell. *Electrochem. Comm.* **2009**, *11*, 457–460.
56. Lee, H.S.; Badami, A.S.; Roy, A.; McGrath, J.E. Segmented sulfonated poly(arylene ether sulfone)-*b*-polyimide copolymers for proton exchange membrane fuel cell. I. Copolymer synthesis and fundamental properties. *J. Polym. Sci. Part A Polym. Chem.* **2007**, *45*, 4879–4890.
57. Yamaki, T.; Tsukada, J.; Asano, M.; Katakai, R.; Yoshida, M. Preparation of highly stable ion exchange membranes by radiation-induced graft copolymerization of styrene and bis(vinyl phenyl)ethane into crosslinked polytetrafluoroethylene films. *J. Fuel Cell Sci. Technol.* **2007**, *4*, 56–64.
58. Meyer, G.; Gebel, G.; Gonon, L.; Capron, P.; Marscaq, D.; Marestin, C.; Mercier, R. Degradation of sulfonated polyimide membranes in fuel cell conditions. *J. Power Sources* **2006**, *157*, 293–301.
59. Aoki, M.; Chikashige, Y.; Miyatake, K.; Uchida, H.; Watanabe, M. Durability of novel sulfonated poly(arylene ether) membrane in PEFC operation. *Electrochem. Comm.* **2006**, *8*, 1412–1416.
60. Gubler, L.; Koppenol, W.H. Kinetic simulation of the chemical stabilization mechanism in fuel cell membranes using cerium and manganese redox couples. *J. Electrochem. Soc.* **2012**, *159*, B211–B218.
61. Gubler, L.; Dockheer, S.M.; Koppenol, W.H. Radical (HO·, H· and HOO·) formation and ionomer degradation in polymer electrolyte fuel cells. *J. Electrochem. Soc.* **2011**, *158*, B755–B769.
62. Nosaka, Y.; Ohtaka, K.; Ohguri, N.; Nosaka, A.Y. Detection of OH radicals generated in polymer electrolyte fuel cells. *J. Electrochem. Soc.* **2011**, *158*, B430–B433.
63. Ohguri, N.; Nosaka, A.Y.; Nosaka, Y. Detection of OH radicals as the effect of Pt particles in the membrane of polymer electrolyte fuel cells. *J. Power Sources* **2010**, *195*, 4647–4652.
64. Gummalla, M.; Atrazhev, V.V.; Condit, D.; Cipollini, N.; Madden, T.; Kuzminyh, N.Y.; Weiss, D.; Burlatsky, S.F. Degradation of polymer-electrolyte membranes in fuel cells II. Theoretical model. *J. Electrochem. Soc.* **2010**, *157*, B1542–B1548.
65. Ohguri, N.; Nosaka, A.Y.; Nosaka, Y. Detection of OH radicals formed at PEFC electrodes by means of a fluorescence probe. *Electrochem. Solid-State Lett.* **2009**, *12*, B94–B96.
66. Franco, A.A.; Guinard, M.; Barthe, B.; Lemaire, O. Impact of carbon monoxide on PEFC catalyst carbon support degradation under current-cycled operating conditions. *Electrochim. Acta* **2009**, *54*, 5267–5279.
67. Inaba, M.; Sugishita, M.; Wada, J.; Matsuzawa, K.; Yamada, H.; Tasaka, A. Impacts of air bleeding on membrane degradation in polymer electrolyte fuel cells. *J. Power Sources* **2008**, *178*, 699–705.
68. Kabasawa, A.; Uchida, H.; Watanabe, M. Influence of decomposition products from perfluorosulfonic acid membrane on fuel cell performance. *Electrochem. Solid-State Lett.* **2008**, *11*, B190–B192.
69. Hommura, S.; Kawahara, K.; Shimohira, T.; Teraoka, Y. Development of a method for clarifying the perfluorosulfonated membrane degradation mechanism in a fuel cell environment. *J. Electrochem. Soc.* **2008**, *155*, A29–A33.

70. Mittal, V.O.; Kunz, H.R.; Fenton, J.M. Membrane degradation mechanisms in PEMFCs. *J. Electrochem. Soc.* **2007**, *154*, B652–B656.
71. Kinumoto, T.; Inaba, M.; Nakayama, Y.; Ogata, K.; Umebayashi, R.; Tasaka, A.; Iriyama, Y.; Abe, T.; Ogumi, Z. Durability of perfluorinated ionomer membrane against hydrogen peroxide. *J. Power Sources* **2006**, *158*, 1222–1228.
72. Aoki, M.; Uchida, H.; Watanabe, M. Decomposition mechanism of perfluorosulfonic acid electrolyte in polymer electrolyte fuel cells. *Electrochem. Comm.* **2006**, *8*, 1509–1513.
73. Inaba, M.; Kinumoto, T.; Kiriake, M.; Umebayashi, R.; Tasaka, A.; Ogumi, Z. Gas crossover and membrane degradation in polymer electrolyte fuel cells. *Electrochim. Acta* **2006**, *51*, 5746–5753.
74. Endoh, E. Highly durable MEA for PEMFC under high temperature and low humidity. *ECS Trans.* **2006**, *3*, 9–18.
75. Aoki, M.; Uchida, M.; Watanabe, M. Novel evaluation method for degradation rate of polymer electrolytes in fuel cells. *Electrochem. Comm.* **2005**, *7*, 1434–1438.
76. Healy, J.; Hayden, C.; Xie, T.; Olson, K.; Waldo, R.; Brundage, M.; Gasteiger, H.; Abbott, J. Aspects of the chemical degradation of PFSA ionomers used in PEM fuel cells. *Fuel Cells* **2005**, *2*, 302–308.
77. Pozio, A.; Silva, R.F.; de Francesco, M.; Giorge, L. Nafion degradation in PEFCs from end plate iron contamination. *Electrochim. Acta* **2003**, *48*, 1543–1549.
78. Huang, C.; Tan, K.S.; Lin, J.; Tan, K.L. XRD and XPS analysis of the degradation of the polymer electrolyte in H₂-O₂ fuel cell. *Chem. Phys. Lett.* **2003**, *371*, 80–85.
79. Delaney, W.E.; Liu, W. Use of FTIR to analyze *ex situ* and *in situ* degradation of perfluorinated fuel cell ionomers. *ECS Trans.* **2007**, *11*, 1093–1104.
80. Endoh, E.; Hommura, S.; Terazono, S.; Wadjaja, H.; Anzai, J. Degradation mechanism of the PFSA membrane and influence of deposited Pt in the membrane. *ECS Trans.* **2007**, *11*, 1083–1091.
81. Curtin, D.E.; Lousenberg, R.D.; Henry, T.J.; Tangeman, P.C.; Tisack, M.E. Advanced materials for improved PEMFC performance and life. *J. Power Sources* **2004**, *131*, 41–48.
82. Zhou, C.; Guerra, M.A.; Qiu, Z.M.; Zawodzinski, T.A., Jr.; Schiraldi, D.A. Chemical durability studies of perfluorinated sulfonic acid polymers and model compounds under mimic fuel cell conditions. *Macromolecules* **2007**, *40*, 8695–8707.
83. Schiraldi, D.A. Perfluorinated polymer electrolyte membrane durability. *J. Macromol. Sci. Part C Polym. Rev.* **2006**, *46*, 315–327.
84. Xie, T.; Hayden, C.A. A kinetic model for the chemical degradation of perfluorinated sulfonic acid ionomers: Weak end group versus side chain cleavage. *Polymer* **2007**, *48*, 5497–5506.
85. Ghassemzadeh, L.; Kreuer, K.D.; Maier, J.; Müller, K. Evaluating chemical degradation of proton conducting perfluorosulfonic acid ionomers in a Fenton test by solid-state ¹⁹F NMR spectroscopy. *J. Power Sources* **2011**, *196*, 2490–2497.
86. Ghassemzadeh, L.; Kreuer, K.D.; Maier, J.; Müller, K. Chemical degradation of Nafion membranes under mimic fuel cell conditions as investigated by solid-state NMR spectroscopy. *J. Phys. Chem. C* **2010**, *114*, 14635–14645.

87. Ghassemzadeh, L.; Morrony, M.; Barrera, R.; Kreuer, K.D.; Maier, J.; Müller, K. Chemical degradation of proton conducting perfluorosulfonic acid ionomer membranes studied by solid-state nuclear magnetic resonance spectroscopy. *J. Power Sources* **2009**, *186*, 334–338.
88. Madden, T.; Weiss, D.; Cipollini, N.; Condit, D.; Gummalla, M.; Burlatsky, S.; Atrazhev, V. Degradation of polymer-electrolyte membranes in fuel cells I. Experimental. *J. Electrochem. Soc.* **2009**, *156*, B657–B662.
89. Fang, X.; Shen, P.K.; Song, S.; Stetgiopoulos, V.; Tsiakaras, P. Degradation of perfluorinated sulfonic acid films: An *in situ* infrared spectro-electrochemical study. *Polym. Degrad. Stab.* **2009**, *94*, 1707–1713.
90. Tang, H.; Peikang, S.; Jiang, S.P.; Wang, F.; Pan, M. A degradation study of Nafion proton exchange membrane of PEM fuel cells. *J. Power Sources* **2007**, *170*, 85–92.
91. Fundamental studies to identify the degradation mechanism of single cell of PEFCs. *Project Annual Report for FYH20 (ID: 100014110)*; Uchimoto, Y. Ed.; 2012. Available online: <http://www.nedo.go.jp/> (accessed on 28 June 2012).
92. Dreizler, A.M.; Roduner, E. Reaction kinetics of hydroxyl radicals with model compounds of fuel cell polymer membranes. *Fuel Cells* **2012**, *12*, 132–140.
93. Serincan, M.F.; Pasaogullari, U. Effect of gas diffusion layer anisotropy on mechanical stresses in a polymer electrolyte membrane. *J. Power Sources* **2011**, *196*, 1314–1320.
94. Shah, A.A.; Luo, K.H.; Ralph, T.R.; Walsh, F.C. Recent trends and developments in polymer electrolyte membrane fuel cell modelling. *Electrochim. Acta* **2011**, *56*, 3731–3757.
95. Serincan, M.F.; Pasaogullari, U.; Molter, T. Modeling the cation transport in an operating polymer electrolyte fuel cell (PEFC). *Int. J. Hydrog. Energy* **2010**, *35*, 5539–5551.
96. Ramousse, J.; Adzakpa, K.P.; Dubé, Y.; Agbossou, K.; Fournier, M.; Poulin, A.; Dostie, M. Local voltage degradations (drying and flooding) analysis through 3D stack thermal modeling. *J. Fuel Cell Sci. Technol.* **2010**, *7*, 041006:1–041006:10.
97. Franco, A.A.; Gerard, M. Multiscale model of carbon corrosion in a PEFC: Coupling with electrocatalysis and impact of performance degradation. *J. Electrochem. Soc.* **2008**, *155*, B367–B384.
98. Franco, A.A.; Tembely, M. Transient multiscale modeling of aging mechanisms in a PEFC cathode. *J. Electrochem. Soc.* **2007**, *154*, B712–B723.
99. Eikerling, M.; Kornyshev, A.; Kulikovskiy, A. Can theory help to improve fuel cells? *Fuel Cell Rev.* **2005**, *1*, 15–25.
100. Wang, C.Y. Fundamental models for fuel cell engineering. *Chem. Rev.* **2004**, *104*, 4727–4766.
101. Fowler, M.W.; Mann, R.F.; Amphlett, J.C.; Peppley, B.A.; Roberge, P.R. Incorporation of voltage degradation into a generalized steady state electrochemical model for a PEM fuel cell. *J. Power Sources* **2002**, *106*, 274–283.
102. Kurniawan, C.; Morita, S.; Kitagawa, K. Hydration structure of trifluoromethanesulfonate studied by quantum chemical calculations. *Comput. Theor. Chem.* **2012**, *982*, 30–33.
103. Ishimoto, T.; Ogura, T.; Koyama, M. Stability and hydration structure of model perfluorosulfonic acid compound systems, $\text{CF}_3\text{SO}_3\text{H}(\text{H}_2\text{O})_n$ ($n = 1-4$), and its isotopomer by the direct treatment of H/D nuclear quantum effects. *Comput. Theor. Chem.* **2011**, *975*, 92–98.

104. Idupulapati, N.; Devanathan, R.; Dupuis, M. Ab initio study of hydration and proton dissociation in ionomer membranes. *J. Phys. Chem. A* **2010**, *114*, 6904–6912.
105. Krishtal, A.; Senet, P.; Alsenoy, C.V. Influence of structure on the polarizability of hydrated methane sulfonic acid clusters. *J. Chem. Theory Comput.* **2008**, *4*, 2122–2129.
106. Vishnyakov, A.; Neimark, A.V. Specifics of solvation of sulfonated polyelectrolytes in water, dimethylmethylphosphonate, and their mixture: A molecular simulation study. *J. Chem. Phys.* **2008**, *128*, 164902:1–164902:11.
107. Koyama, M.; Bada, K.; Sasaki, K.; Tsuboi, H.; Endou, A.; Kubo, M.; Del Carpio, C.A.; Broclawik, E.; Miyamoto, A. First-principles study on proton dissociation properties of fluorocarbon- and hydrocarbon-based membranes in low humidity conditions. *J. Phys. Chem. B* **2006**, *110*, 17872–17877.
108. Urata, S.; Irisawa, J.; Takada, A.; Tsuzuki, S.; Shinoda, W.; Mikami, M. Intermolecular interaction between the pendant chain of perfluorinated ionomer and water. *Phys. Chem. Chem. Phys.* **2004**, *6*, 3325–3332.
109. Paddison, S.J. The modeling of molecular structure and ion transport in sulfonic acid based ionomer membranes. *J. New Mater. Electrochem. Syst.* **2001**, *4*, 197–207.
110. Phonyiem, M.; Chaiwongwattana, S.; Leo-ngam, C.; Sagarik, K. Proton transfer reactions and dynamics of sulfonic acid group in Nafion. *Phys. Chem. Chem. Phys.* **2011**, *13*, 10923–10939.
111. Li, X.; Li, F.; Shi, Y.; Chen, Q.; Sun, H. Predicting water uptake in poly(perfluorosulfonic acids) using force field simulation methods. *Phys. Chem. Chem. Phys.* **2010**, *12*, 14543–14552.
112. Ahadian, S.; Ranjbar, A.; Mizuseki, H.; Kawazoe, Y. A novel computational approach to study proton transfer in perfluorosulfonic acid membranes. *Int. J. Hydrog. Energy* **2010**, *35*, 3648–3655.
113. Choe, Y.K.; Tsuchida, E.; Ikeshoji, T.; Ohira, A.; Kidena, K. An ab initio modeling study on a modeled hydrated polymer electrolyte membrane, sulfonated polyethersulfone (SPES). *J. Phys. Chem. B* **2010**, *114*, 2411–2421.
114. Choe, Y.K.; Tsuchida, E.; Ikeshoji, T.; Yamakawa, S.; Hyodo, S. Nature of proton dynamics in a polymer electrolyte membrane, Nafion: A first-principles molecular dynamics study. *Phys. Chem. Chem. Phys.* **2009**, *11*, 3892–3899.
115. Choe, Y.K.; Tsuchida, E.; Ikeshoji, T.; Yamakawa, S.; Hyodo, S. Nature of water transport and electro-osmosis in Nafion: Insights from first-principles molecular dynamics simulations under an electric field. *J. Phys. Chem. B* **2008**, *112*, 11586–11594.
116. Wilhelm, M.; Jeske, M.; Marschall, R.; Cavalcanti, W.L.; Tölle, P.; Köhler, C.; Koch, D.; Frauenheim, T.; Grathwohl, G.; Caro, J.; Wark, M. New proton conducting hybrid membranes for HT-PEMFC systems based on polysiloxanes and SO₃H-functionalized mesoporous Si-MCM-41 particles. *J. Membr. Sci.* **2008**, *316*, 164–175.
117. Jinnouchi, R.; Okazaki, K. Molecular dynamics study of transport phenomena in perfluorosulfonate ionomer membranes for polymer electrolyte fuel cells. *J. Electrochem. Soc.* **2003**, *150*, E66–E73.
118. Jinnouchi, R.; Okazaki, K. New insight into microscale transport phenomena in PEFC by quantum MD. *Microscale Thermophys. Eng.* **2003**, *7*, 15–31.

119. Clark II, J.K.; Paddison, S.J. The effect of side chain connectivity and local hydration on proton transfer in 3 M perfluorosulfonic acid membranes. *Solid State Ionics* **2012**, *213*, 83–91.
120. Danilczuk, M.; Lin, L.; Schlick, S.; Hamrock, S.J.; Schaberg, M.S. Understanding the fingerprint region in the infra-red spectra of perfluorinated ionomer membranes and corresponding model compounds: Experiments and theoretical calculations. *J. Power Sources* **2011**, *196*, 8216–8224.
121. Li, X.; Liao, S.; Piao, J.; Wang, X. Theoretical study on sulfonated and phosphonated poly[(aryloxy)phosphazene] as proton-conducting membranes for fuel cell applications. *Eur. Polym. J.* **2009**, *45*, 2391–2394.
122. Devanathan, R. Recent developments in proton exchange membranes for fuel cells. *Energy Environ. Sci.* **2008**, *1*, 101–119.
123. Narasimachary, S.P.; Roudgar, A.; Eikerling, M.H. Ab initio study of interfacial correlations in polymer electrolyte membranes for fuel cells at low hydration. *Electrochim. Acta* **2008**, *53*, 6920–6927.
124. Jagur-Grodzinski, J. Polymeric materials for fuel cells: Concise review of recent studies. *Polym. Adv. Technol.* **2007**, *18*, 785–799.
125. Eikerling, M.H.; Malek, K. Physical modeling of materials for PEFCs: A balancing act of water and complex morphologies. In *Proton Exchange Membrane Fuel Cells: Materials Properties and Performance*; Wilkinson, D.P., Zhang, J., Hui, R., Fergus, J., Li, X., Eds.; CRC Press: Florida, FL, USA, 2009; pp. 343–426.
126. Kraka, E.; Cremer, D. Characterization of CF bonds with multiple-bond character: Bond length, stretching force constants, and bond dissociation energies. *Chem. Phys. Chem.* **2009**, *10*, 686–698.
127. Bernardes, C.E.S.; da Piedade, M.E.M.; Amaral, L.M.P.F.; Ferreira, I.M.C.L.; da Silva, A.V.R.; Diogo, H.P.; Cabral, B.J.C. Energies of C–F, C–Cl, C–Br, and C–I bonds in 2-haloethanols, enthalpies of formation of XCH₂CH₂OH (X = F, Cl, Br, I) compounds and of the 2-hydroxyethyl radical. *J. Phys. Chem. A* **2007**, *111*, 1713–1720.
128. Nam, P.C.; Nguyen, M.T.; Chandra, A.K. The C–H and α (C–X) bond dissociation enthalpies of toluene, C₆H₅–CH₂X (X = F, Cl), and their substituted derivatives: A DFT study. *J. Phys. Chem. A* **2005**, *109*, 10342–10347.
129. Izgorodina, E.I.; Coote, M.L.; Radom, L. Trends in R–X bond dissociation energies (R = Me, Et, *i*-Pr, *t*-Bu; X = H, CH₃, OCH₃, OH, F): A surprising shortcoming of density functional theory. *J. Phys. Chem. A* **2005**, *109*, 7558–7566.
130. Coote, M.L.; Pross, A.; Radom, L. Variable trends in R–X bond dissociation energies (R = Me, Et, *i*-Pr, *t*-Bu). *Org. Lett.* **2003**, *5*, 4689–4692.
131. Blanksby, S.L.; Ellison, G.B. Bond dissociation energies of organic molecules. *Acc. Chem. Res.* **2003**, *36*, 255–263.
132. Zavitsas, A.A. The relation between bond lengths and dissociation energies of carbon–carbon bonds. *J. Phys. Chem. A* **2003**, *107*, 897–898.
133. Matsunaga, N.; Rogers, D.W.; Zavitsas, A.A. Pauling’s electronegativity equation and a new corollary accurately predict bond dissociation enthalpies and enhance current understanding of the nature of the chemical bond. *J. Org. Chem.* **2003**, *68*, 3158–3172.

134. Beyer, M. The mechanical strength of a covalent bond calculated by density functional theory. *J. Chem. Phys.* **2000**, *112*, 7307–7312.
135. Pratt, D.A.; Wright, J.S.; Ingold, K.U. Theoretical study of carbon–halogen bond dissociation enthalpies of substituted benzyl halides. How important are polar effects? *J. Am. Chem. Soc.* **1999**, *121*, 4877–4882.
136. Coms, F.D. The chemistry of fuel cell membrane chemical degradation. *ECS Trans.* **2008**, *16*, 235–255.
137. Tokumasu, T.; Ogawa, I.; Koyama, M.; Ishimoto, T.; Miyamoto, A. A DFT study of bond dissociation trends of perfluorosulfonic acid membrane. *J. Electrochem. Soc.* **2011**, *158*, B175–B179.
138. Davi, K.J.; Chandra, A.K. Theoretical investigation of the gas-phase reactions of $(\text{CF}_3)_2\text{CHOCH}_3$ with OH radical. *Chem. Phys. Lett.* **2011**, *502*, 23–28.
139. Jia, X.; Liu, Y.; Sun, J.; Sun, H.; Su, Z.; Pan, X.; Wang, R. Theoretical investigation of the reactions of $\text{CF}_3\text{CHFOCF}_3$ with the OH radical and Cl atom. *J. Phys. Chem. A* **2010**, *114*, 417–424.
140. El-Nahas, A.M.; Uchimaru, T.; Sugie, M.; Tokuhashi, K.; Sekiya, A. Hydrogen abstraction from dimethyl ether (DME) and dimethyl sulfide (DMS) by OH radical: A computational study. *J. Mol. Struct. Theochem.* **2005**, *722*, 9–19.
141. Wu, J.; Liu, J.; Li, Z.; Sun, C. Dual-level direct dynamics studies for the reactions of CH_3OCH_3 and CF_3OCH_3 with the OH radical. *J. Chem. Phys.* **2003**, *118*, 10986–10995.
142. Atadin, F.; Seluki, C.; Sari, L.; Aviyente, V. Theoretical study of hydrogen abstraction from dimethyl ether and methyl tert-butyl ether by hydroxyl radical. *Phys. Chem. Chem. Phys.* **2002**, *4*, 1797–1806.
143. Good, D.A.; Francisco, J.S. Tropospheric oxidation mechanism of dimethyl ether and methyl formate. *J. Phys. Chem. A* **2000**, *104*, 1171–1185.
144. Ishimoto, T.; Nagumo, R.; Ogura, T.; Ishihara, T.; Kim, B.; Miyamoto, A.; Koyama, A. Chemical degradation mechanism of model compound, $\text{CF}_3(\text{CF}_2)_3\text{O}(\text{CF}_2)_2\text{OCF}_2\text{SO}_3\text{H}$, of PFSA polymer by attack of hydroxyl radical in PEMFCs. *J. Electrochem. Soc.* **2010**, *157*, B1305–B1309.
145. Ishimoto, T.; Ogura, T.; Koyama, M. Theoretical study on chemical degradation mechanism of Nafion side chain by the attack of OH radical in polymer electrolyte fuel cell. *J. Electrochem. Soc.* **2011**, *35*, 1–6.
146. Uegaki, R.; Akiyama, Y.; Tojo, S.; Honda, Y.; Nishijima, S. Radical-induced degradation mechanism of perfluorinated polymer electrolyte membrane. *J. Power Sources* **2011**, *196*, 9856–9861.
147. Yu, T.H.; Sha, Y.; Liu, W.G.; Merinov, B.V.; Shirvanian, P.; Goddard, W.A., III. Mechanism for degradation of Nafion in PEM fuel cell from quantum mechanics calculations. *J. Am. Chem. Soc.* **2011**, *133*, 19857–19863.